Effect of guest structure on amylose-guest inclusion complexation

Lingyan Kong – University of Alabama

Diana M. Perez-Santos – Pennsylvania State University

Gregory R. Ziegler – Pennsylvania State University

Citation of published version:

Kong, L., Perez-Santos, D., Ziegler, G. (2018): Effect of guest structure on amylose-guest inclusion complexation. *Food Hydrocolloids*, vol. 97.

DOI: https://doi.org/10.1016/j.foodhyd.2019.105188

Full text at https://doi.org/10.1016/j.foodhyd.2019.105188
or send request to lingyan.kong@ua.edu

Effect of Guest Structure on Amylose-Guest Inclusion Complexation

Lingyan Kong [a], Diana M. Perez-Santos [b, c], and Gregory R. Ziegler [b,*]

[a] Department of Human Nutrition and Hospitality Management, The University of Alabama, Tuscaloosa, AL 35487, USA

[b] Department of Food Science, The Pennsylvania State University, University Park, PA 16802, USA

[c] Centro de Investigacion en Ciencia Aplicada y Tecnologia Avanzada CICATA-IPN, Cerro Blanco No. 141. Col. Colinas del Cimatario. C.P. 76090 Santiago de Queretaro, Queretaro Mexico

[*]Corresponding author. Tel.: (814)863-2960; fax: (814)863-6132. Address: 341 Rodney A. Erickson Food Science Building, University Park, PA 16802, USA

E-mail address: grz1@psu.edu

Abstract: Amylose-guest inclusion complexes are a type of supramolecular host-guest assembly that can provide protection for and controlled release of guest molecules. The successful and efficient complexation between amylose and guest molecules is governed by factors including: guest structure and chemistry, and process method and parameters. Here we investigated the formation, crystalline structure, and thermal stability of amylose inclusion complexes with a total of ten guest molecules differing in alkyl chain length (C10 and C16), molecular shape (linear vs. branched), and functional groups (alcohol, aldehyde, carboxylic acid, and ester). Their ability to complex with amylose was evaluated using two complexation methods (partitioning from water after heating and partitioning from a DMSO/water solution), and two annealing temperatures (60 and 90 °C). The extent of complexation differed for the two methods, likely due to guest solubility and partitioning behavior in the respective solvent systems. Annealing temperature created inclusion complexes of different structure and dissociation temperature using the water approach. Here we suggest that the so-called “Form I” and “Form II” V-type amylose inclusion complexes differ in their crystal size, crystallinity and arrangement of guest molecules in the helical cavity, rather than being amorphous or crystalline as previously reported. Chain length, molecular shape, and functional groups affected the thermal stability of the inclusion complexes. Shorter chain length, unsaturation, and short branched chains formed inclusion complexes with lower dissociation temperatures. We propose the Form II as a tail-to-tail arrangement of molecules in the helices that leaves the functional groups at the helical openings. Guest compounds that either failed to form complexes from water or formed poor complexes were able to form inclusion complexes with amylose using the DMSO approach, suggesting solubility of the guest, flexibility of the amylose chain, or the partitioning of the guest between the solvent and the helix core affected complexation.

Keywords: amylose; starch; inclusion complex; differential scanning calorimetry; X-ray diffraction.

1. Introduction

Supramolecular host-guest assemblies are composed of one compound (the "host") that forms a cavity where molecules of a second "guest" compound are immobilized by interactions through non-covalent bonding. These complex macromolecular architectures can improve the dispersibility and stability, and control release of the guest molecules (Wenz, 2000). Amylose-guest inclusion complexes are a well-known example of host-guest assemblies. A large number of small molecules are known to form host-guest inclusion complexes with amylose, e.g., iodine (Immel & Lichtenthaler, 2000), alcohols (Whittam, et al., 1989), fatty acids and their salts and esters (Fanta, Kenar, Byars, Felker, & Shogren, 2010; Felker, Kenar, Fanta, & Biswas, 2013; Kong & Ziegler, 2014a, 2014b; Lay Ma, Floros, & Ziegler, 2011), salicylic acid and its analogues (Oguchi, Yamasato, Limmatvapirat, Yonemochi, & Yamamoto, 1998; Uchino, Tozuka, Oguchi, & Yamamoto, 2002), and aroma compounds (Nuessli, Putaux, Bail, & Buléon, 2003; Tapanapunnitikul, Chaiseri, Peterson, & Thompson, 2007). Amylose-guest inclusion complexes have attracted interest as encapsulation and delivery systems for certain guest molecules. For instance, conjugated linoleic acid (Lalush, Bar, Zakaria, Eichler, & Shimoni, 2004), genistein (Cohen, Orlova, Kovalev, Ungar, & Shimoni, 2008), fatty acid esters of vitamins and phenolic compounds (Kenar, Compton, Little, & Peterson, 2016; Kong, et al., 2014a, 2014b; Lay Ma, et al., 2011), and long chain unsaturated fatty acids (Lesmes, Barchechath, & Shimoni, 2008; Lesmes, Cohen, Shener, & Shimoni, 2009), have been incorporated into amylose inclusion complexes for encapsulation and release purposes. It is expected that the active ingredients, such as essential fatty acids and lipophilic vitamins, can be protected against adverse environmental factors, e.g., the acidity of the stomach, and therefore stability and bioavailability increased. Through the action of endogenous enzymes or

saccharolytic bacteria, the bioactive guest compounds are then released lower in the gastrointestinal tract (Shimoni, Lesmes, & Ungar, 2010; Tan & Kong, 2019; Yang, Gu, & Zhang, 2009).

Despite the fact that hundreds of compounds have been shown to form inclusion complexes with amylose, a reasonable understanding of the relationship between structural features of guest molecules and the mechanism of complexation is lacking, nor is there a means to predict *a priori* if complexation will occur. A good portion of the literature describes an empirical approach to screening potential guests, while only a few have attempted to relate the complex-forming ability to physicochemical properties or the chemical structure of the guests, e.g., chain length of free fatty acids (Biliaderis, Page, & Maurice, 1986; Le, Choisnard, Wouessidjewe, & Putaux, 2018; Tufvesson, Wahlgren, & Eliasson, 2003), or some readily available thermodynamic properties, e.g., solubility and hydrophilicity (Pozo-Bayon, Biais, Rampon, Cayot, & Le Bail, 2008; Tapanapunnitikul, et al., 2007; Yeo, Thompson, & Peterson, 2016). For example, within the series of monoacylglycerols (1-C10 to 1-C18), Biliaderis, et al. (1986) observed maximum complexation between amylose and monopalmitin (1-C14), suggesting an optimum in the hydrophilicity, but Pozo-Bayon, et al. (2008) evaluated the complexation of 20 aroma compounds and found no correlation between complexing ability and either the chemical class or hydrophobicity expressed as partition coefficient between octane and water (log P), while Yeo, et al. (2016) observed an optimum in complexation at log P of about 2.6-2.8. Kowblansky (1985) studied the complexation of amylose with a variety of straight-chain aliphatic compounds containing 4 to 18 carbons and different functional groups on the terminal carbon and determined that the melting behavior differed between ionic and nonionic functional groups, but the specific nature of the groups had no effect. Recently, Le, et al. (2018) demonstrated that various V-type

92 crystalline allomorphs of amylose-fatty acid inclusion complexes could be obtained by varying
93 fatty acid chain length, fatty acid concentration, crystallization temperature, and solvent
94 composition. It is worthwhile to note that the mechanism of cyclodextrin complexation as
95 affected by guest structure is also, at best, only partly solved and remains open for discussion
96 (Asztemborska & Bielejewska, 2006), despite very diverse and successful practical applications
97 of cyclodextrin inclusion complexes. Hence, in this study, we propose a systematic approach to
98 study amylose-guest complexation, by selecting a range of guest molecules with different chain
99 lengths (C10 and C16), functional groups (alcohol, aldehyde, carboxylic acid, and ester), and
100 molecular shape (linear and branched) (Table 1).

101 Based on the solvent used to dissolve amylose, there are two frequently used methods to
102 prepare amylose-guest inclusion complexes, namely the dimethyl sulfoxide (DMSO) method and
103 high temperature water method (Kong, et al., 2014b). The majority of the aforementioned reports
104 employed the water method to prepare amylose inclusion complexes. This method involves first
105 converting amylose to a molecularly dispersed state by heating to a high temperature (140-
106 160 °C), followed by inclusion of guest molecules at an annealing temperature typically between
107 30 and 90 °C. In the DMSO method, amylose is likewise dissolved in an aqueous DMSO
108 solution (usually 85-100%, v/v DMSO) and mixed with the desired guest. The dispersion is then
109 diluted with water at an annealing temperature (e.g., 60 – 90 °C) and allowed to cool slowly to
110 "room" temperature. It is apparent that the partitioning and complexation of guest compounds
111 also depend on the solvent used in their preparation. For instance, in the water method, the low
112 yield of amylose inclusion complex with long chain fatty acids is likely due to their limited
113 aqueous solubility, while the high hydrophilicity of short chain fatty acids prevents them from
114 partitioning out of the aqueous phase. For complexes formed during differential scanning

calorimetry (DSC), poor mixing in the DSC pans vis-à-vis other water-based methods, e.g., jet cooking (Fanta, Felker, Shogren, & Salch, 2008; Fanta, Kenar, & Felker, 2015), could contribute to the low yield of inclusion complexes using long chain fatty acids. Yet in the DMSO method long chain fatty acids can be effectively complexed due to their higher solubility in DMSO and more effective mixing. Therefore, we employed both methods as certain guest chemistry may favor one over the other.

Here we investigated the thermal and structural properties of amylose inclusion complexes as a function of guest chemistry, solvent environment, and annealing temperature. The thermal stability of the inclusion complexes is associated with their crystalline structure, much of which remains unresolved or under discussion, even for the most extensively studied amylose-lipid inclusion complexes (Le, et al., 2018). Such information will facilitate a fundamental understanding of important interactions between amylose and other food components and improve our ability to prepare functional amylose-guest inclusion complexes.

2. Materials and Methods

2.1. Materials

Amylose from potato starch (degree of polymerization ca. 900), decanol, palmityl alcohol, 2-hexyl-1-decanol, decanal, decanoic acid, palmitic acid, palmitoleic acid, isopropyl palmitate, and glycerol monopalmitate were purchased from Sigma–Aldrich, Inc. (St. Louis, MO). Dimethyl sulfoxide (DMSO), ethanol (200 proof) and palmitic aldehyde were obtained from VWR International (Radnor, PA). Table 1 lists the structures of guest molecules evaluated in this study.

Table 1. Chemical structures of guest molecules evaluated in this study. The naming of compounds per the recommendation of the International Union of Pure and Applied Chemistry (IUPAC), while their common names in parentheses are used in this article.

Chain length (#C)		10	16
Alcohol	Linear	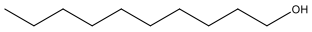 decan-1-ol (decanol)	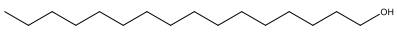 hexadecan-1-ol (palmityl alcohol)
	Branched		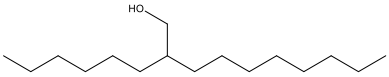 2-hexyldecan-1-ol (2-hexyl-1-decanol)
Aldehyde		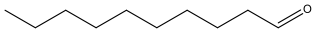 decanal (decanal)	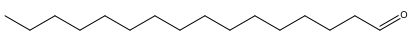 1-hexadecanal (palmitic aldehyde)
Carboxylic acid	Linear alkyl	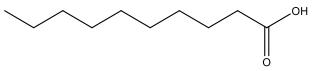 decanoic acid (decanoic acid)	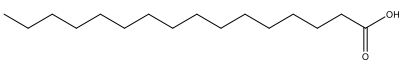 hexadecanoic acid (palmitic acid)
	Unsaturated		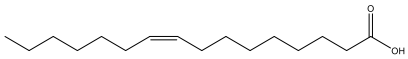 (9Z)-hexadec-9-enoic acid (palmitoleic acid)
Ester			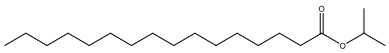 propan-2-yl hexadecanoate (isopropyl palmitate)
			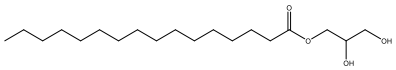 2,3-dihydroxypropyl palmitate (glycerol monopalmitate)

2.2. Preparation of amylose inclusion complexes – water approach

Amylose (5 mg) and guest (0.5 mg) were accurately weighed using a Mettler-Toledo XP2U ultra-microbalance (Mettler-Toledo International Inc., Columbus, OH), water (50 μL) was added

to obtain a 10% (w/v) amylose dispersion, and the dispersion hermetically sealed in large-volume stainless steel DSC pan (Perkin Elmer Co., Norwalk, CT). The pans were equilibrated at room temperature overnight. Amylose-guest inclusion complexation was carried out in a Thermal Advantage Q100 DSC (TA Instruments, New Castle, DE) following the routine: equilibrate at 10 ºC, heat to 150 °C at 10 °C/min, cool to annealing temperature (60 or 90 °C) at 30 °C /min, hold isothermal for 12 h and equilibrate to 25 °C. The DSC was calibrated with indium. An empty sample pan was used as the reference. The wet sample recovered from DSC pans was dried in a desiccator containing Drierite under vacuum and stored for further X-ray diffraction analysis.

2.3. Preparation of amylose inclusion complexes – DMSO approach

Amylose (50 mg) was dissolved in 2 mL of DMSO in a boiling water bath with constant stirring for at least 1 h. The hot amylose dispersion was then cooled to the annealing temperature (60 or 90 °C) and held for 15 min. Guest (5 mg) was added to the dispersion and the sample was kept at the annealing temperature with stirring for another 15 min. Then, 5 mL of water was rapidly added to the sample with vigorous stirring. The sample was incubated with stirring for 30 min at the annealing temperature then allowed to precipitate at room temperature (20 °C) for at least 24 h. The precipitate was recovered by centrifugation (3500 rpm, 20 min), washed twice with 50% (v/v) ethanol/water, and finally with 100% ethanol. The resulting pellet was transferred into an aluminum dish with a small amount of 100% ethanol and allowed to dry at room temperature (20 °C) in a desiccator. Dried samples were pulverized into fine powders for further analysis.

2.4. Wide angle X-ray diffraction (XRD)

Wide angle X-ray diffraction (XRD) patterns were obtained with a Rigaku MiniFlex II X-ray diffractometer (Rigaku Americas Corporation, TX). Samples were exposed to Cu Kα radiation (0.154 nm) and continuously scanned between $2\theta = 4$ and 30 ° at a scanning rate of 1 °/min with a step size of 0.02 °. A current of 15 mA and voltage of 30 kV were used. Data were analyzed by Jade v.8 software (Material Data Inc., Livermore, CA).

2.5. Differential scanning calorimetry (DSC)

Inclusion complex samples made by the water and DMSO approaches were both subject to DSC heating scans, but with different sample preparation procedures. For the water approach, the inclusion complex was prepared in the DSC pan following the protocol described above. For the DMSO approach, approximately 5 to 6 mg of dried inclusion complex sample was weighed using a Mettler-Toledo XP2U ultra-microbalance (Mettler-Toledo International Inc., Columbus, OH) into large-volume stainless steel DSC pans (Perkin Elmer Co., Norwalk, CT) and deionized water was added to obtain a 10% (w/v) sample dispersion. The pan was hermetically sealed and equilibrated at room temperature (20 °C) for at least 2 h. In both instances, thermograms were recorded from 4 to 160 °C at 5 °C/min in a Thermal Advantage Q100 DSC (TA Instruments, New Castle, DE), the samples quenched to 4 °C, then immediately rescanned from 4 to 160 °C at 5 °C/min. Data was analyzed using the TA Universal Analysis software (Universal Analysis 2000 v.4.2E, TA Instruments-Waters LLC, New Castle, DE).

3. Results and Discussion

3.1. Complexation from water

Since water is not a good solvent for amylose, it requires a temperature as high as 160-180 °C to fully dissociate amylose helices and convert them to a random coil state (Creek, Ziegler, & Runt, 2006). Amylose recrystallizes upon cooling, generally in the B crystal form. When guest molecules are introduced into the solution, amylose-guest complexation competes with amylose recrystallization and V-type crystals may form.

3.1.1. Differential scanning calorimetry (DSC)

DSC is a valuable and widely used tool to detect the formation of amylose-guest inclusion complexes. The dissociation of amylose-guest inclusion complexes during heating should produce one or multiple endotherms with peak temperatures generally in the range from 80 to 120 °C, depending mainly on the structure of the inclusion complex. The structure in turn is affected by the guest chemistry and the preparation process. Of the ten non-aromatic guest compounds selected in this study, two guest compounds, 2-hexyl-1-decanol and isopropyl palmitate, did not form inclusion complexes with amylose in water, since no non-negligible endotherm was distinguishable from their DSC thermograms (Fig. S1 in Supplementary Materials). Their inability to form inclusion complexes with amylose by this method could be attributed to their extremely low water solubility (Hoffman & Anacker, 1967; US EPA, 2017). The branched structure of 2-hexyl-1-decanol could also hinder the wrapping by amylose single helices. The other eight guest compounds, including alcohols, aldehydes, carboxylic acids, and esters, formed inclusion complexes at both annealing temperatures, i.e., at 60 and 90 °C, as revealed by endotherms on the DSC thermograms (Fig. 1).

3.1.1.1. Annealing at 60 ºC

Guest compounds with an alkyl chain consisting of 16 carbon atoms produced complexes with higher dissociation temperatures than those with a C10 alkyl chain when annealed at 60 °C. Amylose inclusion complexes with decanal, decanoic acid, and decanol produced endotherms with peak temperatures ranging from 80 to 94 °C, whereas palmitoleic acid, palmitic aldehyde, palmityl alcohol, and palmitic acid complexes generated endotherms with peak temperatures between 100 and 110 °C. Numerous researchers have found that the dissociation temperature of amylose-fatty acid inclusion complexes increases with fatty acid chain length (Biliaderis, et al., 1986; Karkalas, Ma, Morrison, & Pethrick, 1995; Tufvesson, et al., 2003). We recently confirmed this trend by investigating amylose inclusion complexes with 5- and 16-doxyl-stearic acids (Kong, Yucel, Yoksan, Elias, & Ziegler, 2018), and alkylresorcinols (Gunenc, Kong, Elias, & Ziegler, 2018). Molecules with longer hydrocarbon chains allow more hydrophobic interactions with the helix cavity of amylose, and thus will result in inclusion complexes possessing higher dissociation temperatures.

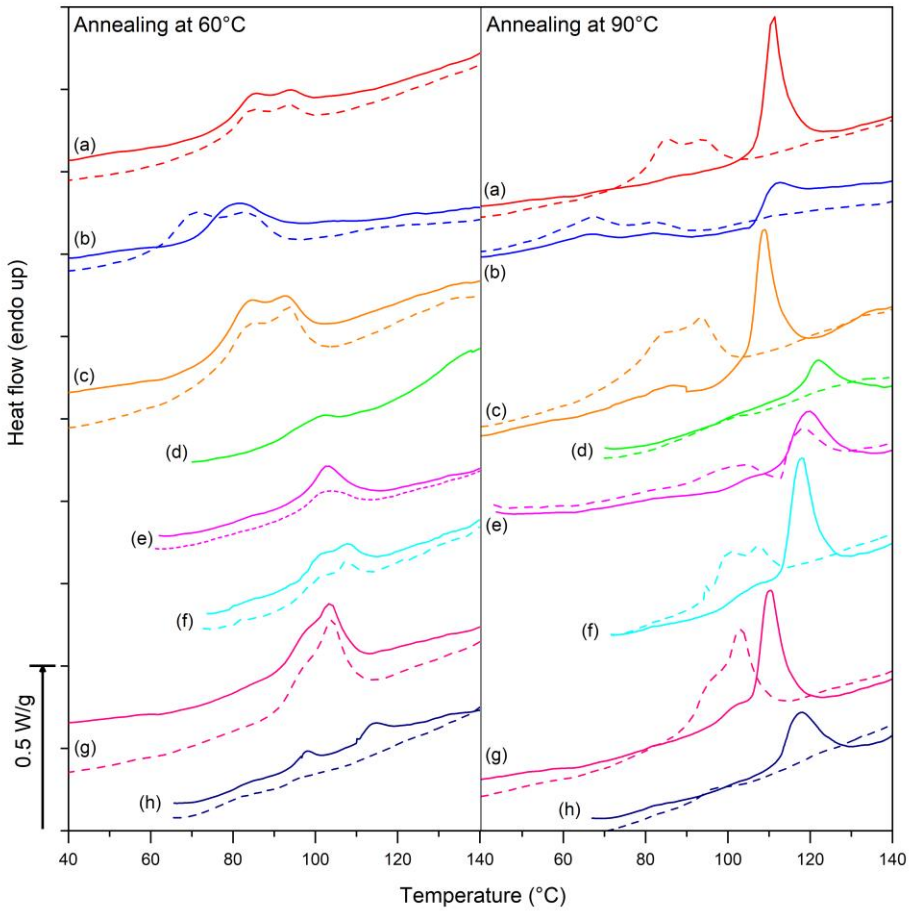

Fig. 1. DSC thermograms of amylose inclusion complexes with (a) decanol, (b) decanal, (c) decanoic acid, (d) palmityl alcohol, (e) palmitic aldehyde, (f) palmitic acid, (g) palmitoleic acid, and (h) glycerol monopalmitate, prepared following the water approach by annealing at 60 °C and 90 °C, respectively. Solid lines denote first heating scan and dashed lines denote second heating scan.

For samples annealed at 60 °C, the second heating scan (dashed lines in Fig. 1), closely approximated the first scans except for decanal, palmityl alcohol and glycerol monopalmitate. A second endotherm at a lower temperature appeared in the amylose-decanal inclusion complex during the second scan making it similar to the other C10 compounds, while amylose-glycerol monopalmitate produced a barely noticeable endotherm on rescan (Fig. 1g) and palmityl alcohol showed no response on rescan (data not shown). By heating to 160 °C during the first scan, guest

molecules were dissociated from the inclusion complex. During the cooling procedure before the second scan, inclusion complexes may be reformed but without an annealing step. Similarity between the first and the second scans implies that annealing at 60 °C did not significantly influence the association between amylose and the guest compounds vis-à-vis no annealing, excepting decanal, palmityl alcohol and glycerol monopalmitate.

Inclusion complexation may not only compete with starch retrogradation, but also with the crystallization of the guest molecules. This was the case for palmityl alcohol, where two large endotherms were observed with peak temperatures at 41 and 54 ºC (not shown in Fig. 1 to avoid cluttering the graphs). Because the melting temperature of glycerol monopalmitate is 60-70 °C (Wang, Peyronel, & Marangoni, 2015), amylose-glycerol monopalmitate might require annealing above 60 °C for the inclusion complex to form, otherwise glycerol monopalmitate might also preferably crystallize with itself, but there was no evidence of this in the XRD pattern (Fig. 2g). Perhaps the annealing time is required to accommodate the bulkier head group.

3.1.1.2. Annealing at 90 ºC

Annealing at 90 °C resulted in complexes with higher transition temperatures vis-à-vis annealing at 60 °C, suggesting a different crystalline organization. The same eight guest molecules complexed with amylose and produced single endotherms with peak temperatures ranging from 108 to 122 °C. Again, inclusion complexes with linear C16 guests, including palmityl alcohol, palmitic aldehyde, palmitic acid, and glycerol monopalmitate, showed higher dissociation temperatures than inclusion complexes with C10 guests, excepting amylose-palmitoleic acid complex, with a peak dissociation temperature closer to those with C10 guests. The existence of a double bond in *cis* conformation distorts amylose helices and results in lower thermal stability for palmitoleic acid complex than that of palmitic acid. Similar effects have

been found in amylose and starch inclusion complexes with other unsaturated fatty acids, e.g., conjugated linoleic acid (Lalush, et al., 2004), and unsaturated alkylresorcinols (Gunenc, et al., 2018).

For samples annealed at 90 °C, the second heating scans did not produce endotherms with the same dissociation temperatures, instead, the samples showed endotherms approximating the second scans of inclusion complexes annealed at 60 °C. For polymorphic crystalline materials, rapid cooling tends to favor the formation of polymorphs with the lowest melting point. The disappearance of the higher temperature endotherms during the second scan suggested that the first heating scan to 160 °C had cleared the "memory effect," i.e. the phenomenon whereby athermal nucleation is observed in a cooled melt after heating above the melting temperature, of the Form II inclusion complexes (defined in the following discussion). This phenomenon was observed in polymer systems, such as agarose and amylose gelation, during recrystallization or reassociation due to unmelted nuclei above the melting temperature leading to crystal growth upon cooling (Creek, et al., 2006). Here, although annealing at 90 °C resulted in crystalline structures of higher thermal stability, the structures formed appeared to be destroyed by melting the helical nuclei to 160 ºC.

3.1.2. X-ray diffraction (XRD)

When complexed with guest compounds amylose forms left-handed single helices with a central cavity wrapping the guest that can then crystallize in the V-type structure. Depending on the size and shape of the guest molecule, various subtypes of V can be formed. With aliphatic guest compounds amylose usually crystallizes into the V type containing 6 glucose units per helical turn (V_6). The V_6 structure can be further categorized as the hydrated V_6 (V_{6h}) with characteristic X-ray diffraction peaks at about 7.5°, 13° and 20°, or the anhydrous V_6 (V_{6a}) with

characteristic X-ray diffraction peaks at 7.8°, 13.5° and 21°. Amylose inclusion complexes with seven of the guest compounds in Fig. 1 all showed evidence of V_6 type diffraction peaks (Fig. 2), although some with low peak intensities and the additional presence of B-type crystals with characteristic peaks at about 17°, 22°, and 24° (e.g., at 60 ºC, d & e and at 90 ºC, d & g). XRD showed strong peaks for crystalline palmityl alcohol and the presence of B-type amylose crystallinity that obscured peaks for V-type in that sample (for clarity this data is not presented in Fig. 2).

In general, inclusion complexes annealed at 90 °C showed sharper diffraction peaks and higher crystallinity than those annealed at 60 °C (Fig. 2). A clearer comparison in the case of decanol and decanoic acid can be found in Fig. S3 in Supplementary Materials. The implications of the peak sharpness and crystallinity will be further discussed in subsection 3.1.3.

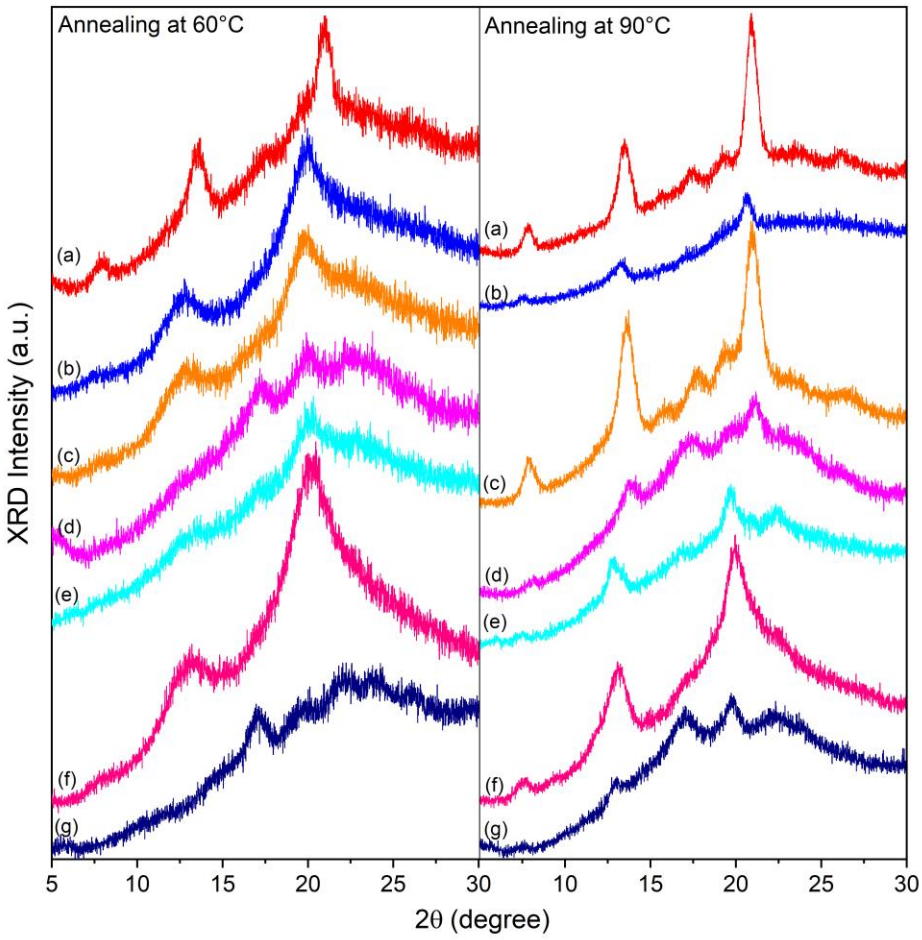

Fig. 2. XRD patterns of amylose inclusion complexes with (a) decanol, (b) decanal, (c) decanoic acid, (d) palmitic aldehyde, (e) palmitic acid, (f) palmitoleic acid, and (g) glycerol monopalmitate, prepared following the water approach by annealing at 60 °C and 90 °C, respectively.

3.1.3. Crystalline structure model

The observation of multiple dissociation temperatures implies the existence of different crystalline structures of amylose inclusion complexes, further complicating the endeavor to elucidate the V-type amylose microstructure. First proposed by Biliaderis and Galloway (1989), two separate thermodynamic states, i.e., type-I and type-II, of amylose inclusion complexes could be formed depending on crystallization temperature (Fig. 3A); 60 ºC and lower results in

type-I while 90 ºC or higher produces type-II (Goderis, Putseys, Gommes, Bosmans, and Delcour, 2014). Biliaderis, et al. (1989) suggested type-I was a random distribution of helical elements formed by rapid nucleation at low "crystallization" temperatures, whereas the type-II was described as a partially crystalline structure obtained at higher "crystallization" temperatures or by conversion from type-I via a partial melting and recrystallization. This theory has been widely accepted yet is inconsistent with some experimental observations. For instance, some guests result in only type I complexes as defined by dissociation temperature (e.g., lysophosphatidylcholine) (Biliaderis, Page, Slade, & Sirett, 1985), and some of these type I complexes show X-ray diffraction patterns as good or better than those of type II (Marinopoulou, Papastergiadis, Raphaelides, & Kontominas, 2016; Shimoni, et al., 2010).

Recently, Goderis, et al. (2014) proposed that all types of amylose-glycerol monostearate inclusion complexes consist of crystallized single helices with differences in lamellar layer thickness and number of lipid molecules within the helices (Fig. 3B). This model involves the alignment of multiple glycerol monostearate molecules within the V_6 type amylose helix. A similar model involving linear arrangement of two fatty acids in the V_6 type amylose helix, particularly with two carboxyl groups meeting inside (Fig. 3C) was proposed by Shogren, Fanta, and Felker (2006). However, others have concluded that the amylose helical cavity is not capable of accommodating hydroxyl, carboxyl or glycerol groups due to hydrophilicity and/or size (Carlson, Larsson, Dinh‐Nguyen, & Krog, 1979; Godet, Buleon, Tran, & Colonna, 1993; Godet, Tran, Delage, & Buléon, 1993; Nimz, Gessler, Usón, Sheldrick, & Saenger, 2004). The arrangement of guest molecules in amylose helices and the localization of the functional groups are still under discussion. Herein we designate the inclusion complexes with lower dissociation temperatures, e.g., as formed either by annealing at 60 °C or without annealing, as Form I (Form

Ia and Form Ib if occurring as a doublet), while those with higher dissociation temperatures formed by annealing at 90 °C as Form II (Fig. 3D).

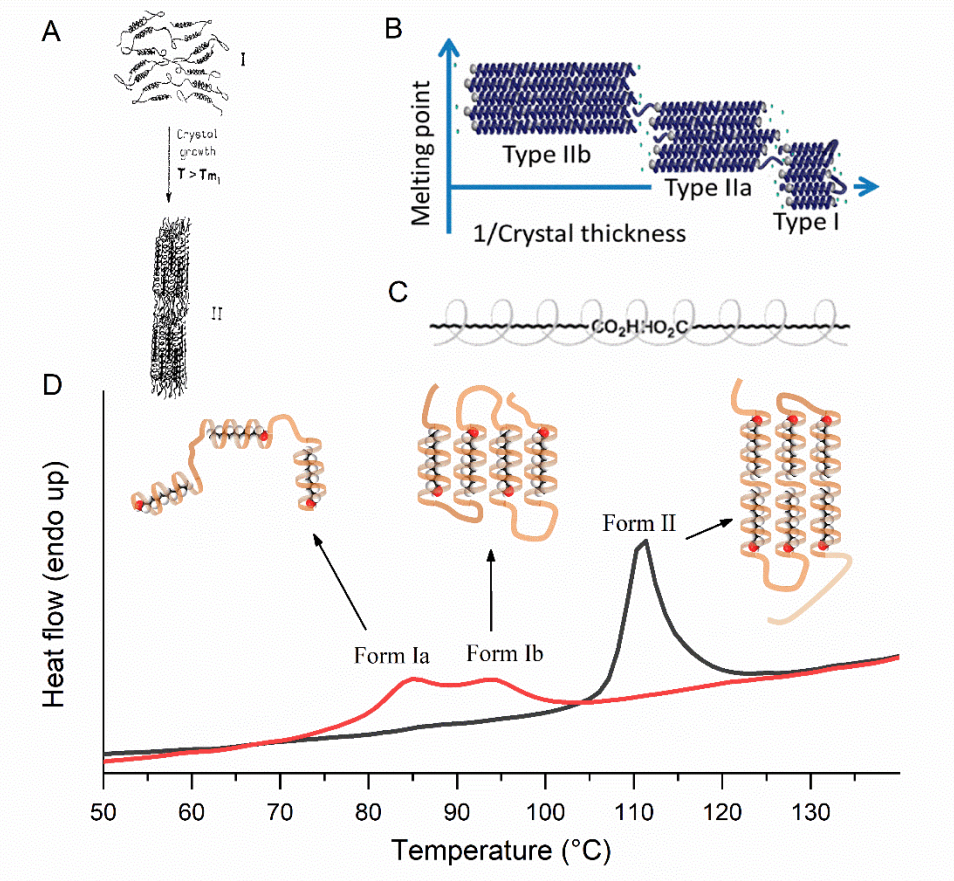

Fig. 3. Structures of Form I and II V-type amylose inclusion complex proposed by (A) Biliaderis, et al. (1989), reprinted with permission from Elsevier; (B) Goderis, et al. (2014), reprinted with permission from American Chemical Society; (C) Shogren, et al. (2006) reprinted with permission from Elsevier; and (D) this study using amylose-decanol inclusion complex as the model.

Among both forms of amylose inclusion complexes, the effect of alkyl chain length on dissociation temperature was expected since longer alkyl chains facilitate stronger hydrophobic interaction with the amylose helical channel and thus render higher dissociation temperatures. Tufvesson, et al. (2003) reported that the dissociation temperatures of both forms increased with

fatty acid chain length with well-fitted linear relationships, suggesting crystal or lamellar thickness contributed to the heat stability as measured by the dissociation temperature of amylose inclusion complexes. By direct microscopic measurement of crystalline complexes formed by amylose (DP 900) and fatty acids with 8, 12 or 16 carbons, Godet, Bouchet, Colonna, Gallant, and Buleon (1996) found that the crystal lamellar thickness never exceeded 4.6 nm corresponding to the total length of two palmitic acid molecules and concluded that a maximum of two fatty acid molecules could be included in the lamellae with carboxylic groups outside the crystallite in amorphous regions, a result in direct contradiction of Goderis, et al. (2014) (Fig. 3B). According to Godet, Bizot, and Buléon (1995), these amylose-palmitic acid inclusion complexes had a dissociation temperature range of 105-120 ºC and, therefore, would be Form II as we designate here (Fig. 3D). Furthermore, inclusion of the carboxyl group would likely result in the formation of 7-fold instead of the 6-fold helices (Le, et al., 2018) making the arrangement in Fig. 3B & 3C unlikely in the present case.

From the results of this study, we propose the Form I as a combination of non-crystalline (Form Ia) and crystalline (Form Ib) inclusion complexes with one alkyl chain residing in one helical segment, and the Form II as two guest molecules residing in the helical channel of the inclusion complex with a tail-to-tail arrangement (Fig. 3D). The Form Ia consists of randomly-oriented helical segments, while the Form Ib represents the typical V-type antiparallel packing with guest molecules alternating direction of functional groups. The presence of both forms Ia and Ib simultaneously resulting in the rather poor XRD patterns typically observed for Form I. Therefore, Form Ib is more thermally stable than Form Ia, as evidenced by a slightly higher dissociation temperature.

Biomodal endotherms were recorded while varying the heating rate from 0.5 °C/min to 10 °C/min for Form I amylose-decanol complexes formed by annealing at 60 ºC (Fig. S2 in Supplementary Materials). As the heating rate increased, the proportion of Form Ib decreased (Fig. S2 inset), implying that a transition from Form Ia to Form Ib occurred during heating in the DSC. This transition is consistent with the model proposed in Fig. 3. Apparently rapid complex formation caused by deeper undercooling (60 °C) or the absence of annealing (on rescan) trapped complexes in a mixture of Forms Ia, and Form Ib as observed in Fig. 1 and supported by XRD (Fig. 2). The exception was decanal that revealed only Form Ib on annealing at 60 °C (Fig. 1). In this case the annealing temperature (60 °C) corresponded to the onset of dissociation of Form Ia (peak dissociation temperature 71 ºC), which provided enough mobility for the transition to Form Ib to occur during annealing. A transition from Form I to Form II was not observed, even at the slowest heating rate, suggesting there was not enough time in the narrow temperature range between the conclusion temperature for dissociation of Form I and the onset temperature for dissociation of Form II. Goderis, et al. (2014) did note a short time window between the melting of Form I and crystallization of Form II where the material was amorphous.

The Form II has even higher dissociation temperature due to thicker lamellae and larger crystal size. Unlike the model proposed by Shogren, et al. (2006), the suggested tail-to-tail arrangement herein excludes the relatively hydrophilic and bulky functional groups from the center of the amylose helices. For both the C10 and C16 series, the dissociation temperatures for Form II followed the order alcohol>aldehyde>acid (Fig. 1. 90 ºC a>b>c and d>e>f), i.e., as the guest head group became larger or more highly charged it was excluded to a greater extent from the helix, resulting in lesser interaction with the alkyl tail and a lower dissociation temperature. Other researchers suggested that polar groups larger than the size of a carboxyl group are located

outside of the helical cavity (Snape, Morrison, Maroto-Valer, Karkalas, & Pethrick, 1998), which is consistent with our observation of the lowest dissociation temperature in the C16:0 series for glycerol monopalmitate (Fig. 1. 90 ºC h). However, Marinopoulou, et al. (2016) proposed fringed micelle and folded lamellae structures that included the headgroup both outside and within the helices. Although we hypothesized the tail-to-tail arrangement, the localization and orientation of functional groups at the end of the alkyl chain is a topic requiring further investigation and discussion (Kong, et al., 2018). Annealing at 90 °C apparently resulted in a larger crystallite size indicated by a smaller full width at half maximum (FWHM) on X-ray diffraction peaks. The higher enthalpies of melting in Form II inclusion complexes in Fig. 1 and Fig. S3 should be the result of higher total crystallinity in the samples.

3.2. Complexation from DMSO/water

For the four compounds that either failed to form complexes from water, i.e., 2-hexyl-1-decanol and isopropyl palmitate, or formed complexes poorly, i.e., palmityl alcohol and glycerol monopalmitate, we hypothesized this was due to limited contact between the starch and guest compound due either to poor water solubility or a lack of stirring in the DSC pans. DMSO is a good solvent for amylose and for fatty acids and increases the availability of weakly soluble fatty acids for complexation (Le, et al., 2018). Therefore, we employed the DMSO method to form complexes from these guest compounds (Fig. 4).

By annealing at both 60 °C and 90 °C, amylose-palmityl alcohol complexes readily formed with a peak dissociation temperature just under 100 ºC (Fig. 4a). A doublet appeared on rescan like that for Form-I complexes. Form-II complexes with a melting point above 120 ºC (Fig. 1) were not observed for complexes made by the DMSO method. XRD revealed a V_6 pattern as expected for Form-I complexes. Similar dissociation temperatures and V_6 patterns were observed

for amylose-glycerol monopalmitate inclusion complexes formed by annealing at 60 and 90 °C. In both thermograms, the peak endothermic temperatures ranged between 90-100 °C in the first scans and rescans (Fig. 4d), which were close to the dissociation temperature of the Form-I complex formed by the water method at 60 °C. Yet, much better resolved V_6 patterns could be obtained by the DMSO method than in the water method.

V_6 amylose-isopropyl palmitate complexes formed on cooling after an annealing temperature of 90 ºC but not at 60 ºC (Fig. 4c). The peak dissociation temperature was just under 80 ºC but the conclusion temperature exceeded 95 ºC. Similarly, Goderis, et al. (2014) observed rapid formation of complexes on cooling amylose-glycerol monostearate complexes to 70 ºC after an isothermal hold at 110 ºC and concluded that nucleation of complexes occurred at the higher temperature followed by rapid growth on cooling.

The dissociation temperature of amylose-2-hexyl-1-decanol inclusion complex produced by annealing at 90 °C was around 60 °C (Fig. 4b), much lower than other inclusion complexes. We argue that the branched structure of 2-hexyl-1-decanol interfered with regular helical wrapping by amylose, distorting the amylose helix. But the linear portions of this molecule, i.e., the C6 and C8 branches, may complex with amylose, and the DMSO approach seemed to facilitate this complexation. With these short branches forming the inclusion complex, the dissociation temperature was accordingly lower than the amylose-C10 inclusion complexes. Similar results were seen in amylose inclusion complexes with other branched molecules, such as 5-doxyl-stearic acid (Kong, et al., 2018), where the doxyl ring group at C5 position divides the stearic acid molecule into two branches consisting of 5 and 13 carbon atoms, respectively. As a result, the dissociation temperature of amylose-5-doxyl-stearic acid inclusion complex was lower than amylose-stearic acid inclusion complex. Amylose-2-hexyl-1-decanol formed inclusion

complexes on cooling after annealing at 60 ºC exhibiting two small endotherms with peaks at 80 and 100 ºC (Fig. 4), which could possibly be due to a more rigid extended conformation of the guest molecule at the lower temperature, yielding a Form-I complex similar to that of palmityl alcohol and glycerol monopalmitate though to a much lower extent.

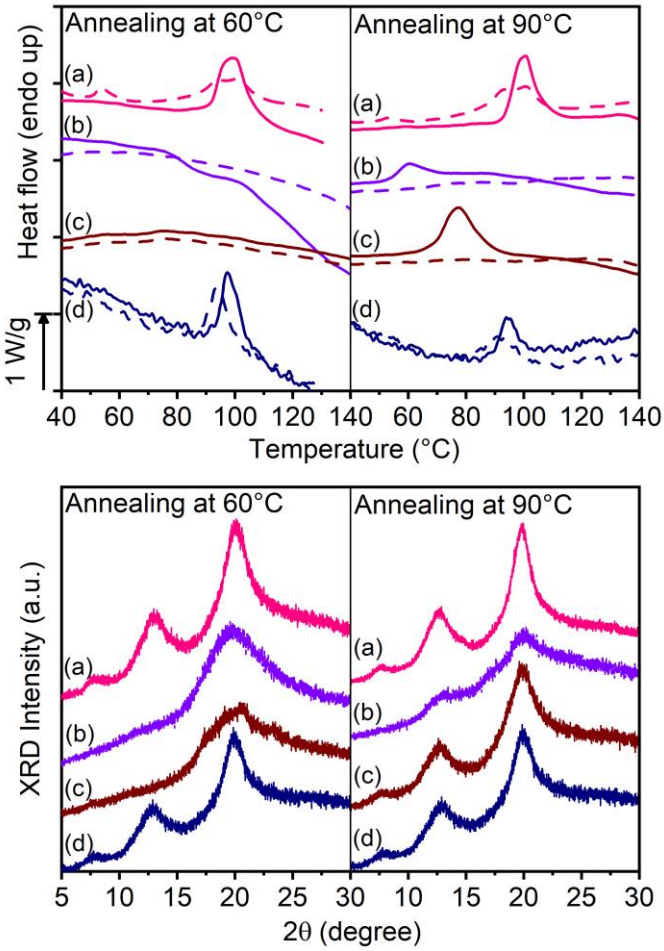

Fig. 4. DSC thermograms and XRD patterns of amylose inclusion complexes with (a) palmityl alcohol (b) 2-hexyl-1-decanol (c) isopropyl palmitate, and (d) glycerol monopalmitate prepared following the DMSO approach by annealing at 60 °C and 90 °C, respectively. In DSC thermograms, solid lines denote first heating scan and dashed lines denote second heating scan.

DMSO not only alters the solubility of the guest, but also the flexibility of the amylose chain and the partitioning of the guest between the solvent and the helix core. Apparently one or

more of these factors affected the inclusion of guest compounds from DMSO such that only Form-I complexes were formed at either annealing temperature.

4. Conclusions

In conclusion, the formation, structure, and thermal properties of inclusion complexes between amylose and a pool of ten guest compounds, which varied systematically in their structure and chemistry, were studied using two complexation methods and two annealing temperatures. The alkyl chain length mainly affected the dissociation temperature of the amylose-guest inclusion complexes; C16 guests formed inclusion complexes with higher dissociation temperatures than C10 guests. The functional groups on the aliphatic chain affected the structure and dissociation temperature of inclusion complexes. We proposed a model for structures of Form Ia, Ib, and Form II as non-crystalline helices, crystalline V-type helical packing with one alkyl chain residing in one helical segment, and the tail-to-tail arrangement of two guest molecules in the helices with functional groups at the helical openings, respectively. Considerable work remains to elucidate the V-complex structure formed by more complex guests, e.g. cyclic molecules, and those that result in helices with greater than 6 glucose units. We also propose to study the mechanism in a more efficient complexation method, the preformed “empty” helical method (Kong, et al., 2014b).

Supplementary Materials

Fig. S1. DSC thermograms of amylose inclusion complexes with (a) isopropyl palmitate and (b) 2-hexyl-1-decanol, prepared following the water approach by annealing at 60 °C (solid lines) and 90 °C (dashed lines), respectively.

Fig. S2. DSC thermograms of amylose-decanol inclusion complex scanned at varying heating rate. Dotted lines show deconvolution of the endotherms and inlet shows the relative percentage

area of the second endotherm with respect to the total area under curve as a function of heating rate.

Fig. S3. DSC thermograms and XRD patterns of amylose inclusion complexes with (a) decanol and (b) decanoic acid, prepared following the water approach by annealing at 60 °C (left) and 90 °C (right), respectively.

Acknowledgment

This work was supported by the USDA National Institute for Food and Agriculture, National Competitive Grants Program, National Research Initiative Program 71.1 FY 2007 as grant # 2007-35503-18392. This work is/was supported by the USDA National Institute of Food and Agriculture and Hatch Appropriations under Project #PEN04565 and Accession #1002916.

References

Asztemborska, M., & Bielejewska, A. (2006). Chromatographic Studies of Molecular and Chiral Recognition. In H. Dodziuk (Ed.), *Cyclodextrins and Their Complexes* (pp. 106-118). Weinheim: Wiley.

Biliaderis, C. G., & Galloway, G. (1989). Crystallization behavior of amylose-V complexes: Structure-property relationships. *Carbohydrate Research, 189*, 31-48.

Biliaderis, C. G., Page, C. M., & Maurice, T. J. (1986). Non-equilibrium melting of amylose-V complexes. *Carbohydrate Polymers, 6*, 269-288.

Biliaderis, C. G., Page, C. M., Slade, L., & Sirett, R. R. (1985). Thermal behavior of amylose-lipid complexes. *Carbohydrate Polymers, 5*, 367-389.

Carlson, T. G., Larsson, K., Dinh‐Nguyen, N., & Krog, N. (1979). A study of the amylose‐monoglyceride complex by Raman spectroscopy. *Starch‐Stärke, 31*, 222-224.

Cohen, R., Orlova, Y., Kovalev, M., Ungar, Y., & Shimoni, E. (2008). Structural and functional properties of amylose complexes with genistein. *Journal of Agricultural and Food Chemistry, 56*, 4212-4218.

Creek, J. A., Ziegler, G. R., & Runt, J. (2006). Amylose crystallization from concentrated aqueous solution. *Biomacromolecules, 7*, 761-770.

Fanta, G. F., Felker, F. C., Shogren, R. L., & Salch, J. H. (2008). Preparation of spherulites from jet cooked mixtures of high amylose starch and fatty acids. Effect of preparative conditions on spherulite morphology and yield. *Carbohydrate Polymers, 71*(2), 253-262.

Fanta, G. F., Kenar, J. A., Byars, J. A., Felker, F. C., & Shogren, R. L. (2010). Properties of aqueous dispersions of amylose–sodium palmitate complexes prepared by steam jet cooking. *Carbohydrate Polymers, 81*, 645-651.

Fanta, G. F., Kenar, J. A., & Felker, F. C. (2015). Nanoparticle formation from amylose-fatty acid inclusion complexes prepared by steam jet cooking. *Industrial Crops and Products, 74*, 36-44.

Felker, F. C., Kenar, J. A., Fanta, G. F., & Biswas, A. (2013). Comparison of microwave processing and excess steam jet cooking for spherulite production from amylose‐fatty acid inclusion complexes. *Starch ‐ Stärke, 65*(9 ‐ 10), 864-874.

Goderis, B., Putseys, J. A., Gommes, C. d. J., Bosmans, G. M., & Delcour, J. A. (2014). The structure and thermal stability of amylose–lipid complexes: A case study on amylose–glycerol monostearate. *Crystal Growth & Design, 14*, 3221-3233.

Godet, M. C., Bizot, H., & Buléon, A. (1995). Crystallization of amylose—fatty acid complexes prepared with different amylose chain lengths. *Carbohydrate Polymers, 27*, 47-52.

Godet, M. C., Bouchet, B., Colonna, P., Gallant, D. J., & Buleon, A. (1996). Crystalline amylose-fatty acid complexes: morphology and crystal thickness. *Journal of Food Science, 61*, 1196-1201.

Godet, M. C., Buleon, A., Tran, V., & Colonna, P. (1993). Structural features of fatty acid-amylose complexes. *Carbohydrate Polymers, 21*, 91-95.

Godet, M. C., Tran, V., Delage, M. M., & Buléon, A. (1993). Molecular modelling of the specific interactions involved in the amylose complexation by fatty acids. *International Journal of Biological Macromolecules, 15*, 11-16.

Gunenc, A., Kong, L., Elias, R. J., & Ziegler, G. R. (2018). Inclusion complex formation between high amylose corn starch and alkylresorcinols from rye bran. *Food chemistry, 259*.

Hoffman, C. S., & Anacker, E. W. (1967). Water solulbilities of tetradecanol and hexadecanol. *Journal of Chromatography A, 30*, 390-396.

Immel, S., & Lichtenthaler, F. W. (2000). The hydrophobic topographies of amylose and its blue iodine complex. *Starch - Stärke, 52*, 1-8.

Karkalas, J., Ma, S., Morrison, W. R., & Pethrick, R. A. (1995). Some factors determining the thermal properties of amylose inclusion complexes with fatty acids. *Carbohydrate Research, 268*, 233-247.

Kenar, J. A., Compton, D. L., Little, J. A., & Peterson, S. C. (2016). Formation of inclusion complexes between high amylose starch and octadecyl ferulate via steam jet cooking. *Carbohydrate Polymers, 140*, 246-252.

Kong, L., Yucel, U., Yoksan, R., Elias, R. J., & Ziegler, G. R. (2018). Characterization of amylose inclusion complexes using electron paramagnetic resonance spectroscopy. *Food Hydrocolloids, 82*, 82-88.

Kong, L., & Ziegler, G. R. (2014a). Formation of starch-guest inclusion complexes in electrospun starch fibers. *Food Hydrocolloids, 38*, 211-219.

Kong, L., & Ziegler, G. R. (2014b). Molecular encapsulation of ascorbyl palmitate in preformed V-type starch and amylose. *Carbohydrate Polymers, 111*, 256-263.

Kowblansky, M. (1985). Calorimetric investigation of inclusion complexes of amylose with long-chain aliphatic compounds containing different functional groups. *Macromolecules, 18*, 1776-1779.

Lalush, I., Bar, H., Zakaria, I., Eichler, S., & Shimoni, E. (2004). Utilization of amylose−lipid complexes as molecular nanocapsules for conjugated linoleic acid. *Biomacromolecules, 6*, 121-130.

Lay Ma, U. V., Floros, J. D., & Ziegler, G. R. (2011). Formation of inclusion complexes of starch with fatty acid esters of bioactive compounds. *Carbohydrate Polymers, 83*, 1869-1878.

Le, C.-A.-K., Choisnard, L., Wouessidjewe, D., & Putaux, J.-L. (2018). Polymorphism of crystalline complexes of V-amylose with fatty acids. *International Journal of Biological Macromolecules, 119*, 555-564.

Lesmes, U., Barchechath, J., & Shimoni, E. (2008). Continuous dual feed homogenization for the production of starch inclusion complexes for controlled release of nutrients. *Innovative Food Science and Emerging Technologies, 9*, 507-515.

Lesmes, U., Cohen, S. H., Shener, Y., & Shimoni, E. (2009). Effects of long chain fatty acid unsaturation on the structure and controlled release properties of amylose complexes. *Food Hydrocolloids, 23*, 667-675.

Marinopoulou, A., Papastergiadis, E., Raphaelides, S. N., & Kontominas, M. G. (2016). Structural characterization and thermal properties of amylose-fatty acid complexes prepared at different temperatures. *Food Hydrocolloids, 58*, 224-234.

Nimz, O., Gessler, K., Usón, I., Sheldrick, G. M., & Saenger, W. (2004). Inclusion complexes of V-amylose with undecanoic acid and dodecanol at atomic resolution: X-ray structures with cycloamylose containing 26 d-glucoses (cyclohexaicosaose) as host. *Carbohydrate Research, 339*, 1427-1437.

Nuessli, J., Putaux, J. L., Bail, P. L., & Buléon, A. (2003). Crystal structure of amylose complexes with small ligands. *International Journal of Biological Macromolecules, 33*, 227-234.

Oguchi, T., Yamasato, H., Limmatvapirat, S., Yonemochi, E., & Yamamoto, K. (1998). Structural change and complexation of strictly linear amylose induced by sealed-heating with salicylic acid. *Journal of the Chemical Society, Faraday Transactions, 94*, 923-927.

Pozo-Bayon, M. A., Biais, B., Rampon, V., Cayot, N., & Le Bail, P. (2008). Influence of complexation between amylose and a flavored model sponge cake on the degree of aroma compound release. *Journal of Agricultural and Food Chemistry, 56*, 6640-6647.

Shimoni, E., Lesmes, U., & Ungar, Y. (2010). Non-covalent complexes of bioactive agents with starch for oral delivery. US Patent Application 2010/0008982.

Shogren, R. L., Fanta, G. F., & Felker, F. C. (2006). X-ray diffraction study of crystal transformations in spherulitic amylose/lipid complexes from jet-cooked starch. *Carbohydrate Polymers, 64*, 444-451.

Snape, C. E., Morrison, W. R., Maroto-Valer, M. M., Karkalas, J., & Pethrick, R. A. (1998). Solid state 13C NMR investigation of lipid ligands in V-amylose inclusion complexes. *Carbohydrate Polymers, 36*, 225-237.

Tan, L., & Kong, L. (2019). Starch-guest inclusion complexes: Formation, structure, and enzymatic digestion. *Critical reviews in food science and nutrition*, 1-11. DOI: 10.1080/10408398.10402018.11550739.

Tapanapunnitikul, O., Chaiseri, S., Peterson, D. G., & Thompson, D. B. (2007). Water solubility of flavor compounds influences formation of flavor inclusion complexes from dispersed high-amylose maize starch. *Journal of Agricultural and Food Chemistry, 56*, 220-226.

Tufvesson, F., Wahlgren, M., & Eliasson, A. C. (2003). Formation of amylose-lipid complexes and effects of temperature treatment. Part 2. fatty acids. *Starch - Stärke, 55*, 138-149.

Uchino, T., Tozuka, Y., Oguchi, T., & Yamamoto, K. (2002). Inclusion compound formation of amylose by sealed-heating with salicylic acid analogues. *Journal of Inclusion Phenomena and Macrocyclic Chemistry, 43*, 31-36.

US EPA. (2017). *Estimation Programs Interface Suite™ for Microsoft® Windows, v 4.11. United States Environmental Protection Agency, Washington, DC, USA.*

Wang, F. C., Peyronel, F., & Marangoni, A. G. (2015). Phase diagram of glycerol monostearate and sodium stearoyl lactylate. *Crystal Growth & Design, 16*, 297-306.

Wenz, G. (2000). An overview of host-guest chemistry and its application to nonsteroidal anti-inflammatory drugs. *Clinical Drug Investigation, 19*, 21-25.

Whittam, M. A., Orford, P. D., Ring, S. G., Clark, S. A., Parker, M. L., Cairns, P., & Miles, M. J. (1989). Aqueous dissolution of crystalline and amorphous amylose-alcohol complexes. *International Journal of Biological Macromolecules, 11*, 339-344.

Yang, Y., Gu, Z., & Zhang, G. (2009). Delivery of bioactive conjugated linoleic acid with self-assembled amylose−CLA complex. *Journal of Agricultural and Food Chemistry, 57*, 7125-7130.

Yeo, L., Thompson, D. B., & Peterson, D. G. (2016). Inclusion complexation of flavour compounds by dispersed high-amylose maize starch (HAMS) in an aqueous model system. *Food chemistry, 199*, 393-400.